

Thermal Conductivity of Filled Silicone Rubber and its Relationship to Erosion Resistance in the Inclined Plane Test

Luiz Meyer, Shesha Jayaram and Edward A. Cherney

University of Waterloo, 200 University Av. W.
Waterloo, N2L 3G1, Ontario, Canada

ABSTRACT

Silicone rubber samples having various concentrations and mean particle sizes of either alumina tri-hydrate or silica fillers, prepared by room temperature and heat cured under pressure (hot pressed), are tested for erosion resistance in the ASTM D2303 inclined plane tracking and erosion test. Their corresponding thermal conductivities are determined using a transient temperature technique in which an infrared laser is employed as the heat source and a thermal imaging camera as a temperature detection device. Scanning electron microscope observations show greater filler bonding to the silicone matrix in the hot pressed samples than in the room temperature vulcanized samples leading higher thermal conductivity and increased resistance to erosion, for both ATH and silica filled samples. The correlation study shows a strong relationship between the erosion resistance and the thermal conductivity of the tested samples, highlighting the importance of an outdoor insulating material to have high thermal conductivity in order to withstand dry band arcing. The results can be used to provide guidance on filler selection for silicone rubber compounding for outdoor insulation applications.

Index Terms — Thermal conductivity of silicone rubber, erosion resistance of filled silicone rubber, inclined plane tracking and erosion test of filled silicone rubber.

1 INTRODUCTION

POLYMERIC high voltage insulators have been in use on distribution and transmission lines for more than 25 years and are increasingly replacing glass and porcelain insulators around the world. Their light weight is an attractive feature of these insulators as this manifests itself in a lower installation cost, easier handling and less damage during transport when compared to ceramic insulators. Polymeric insulators with weathersheds made from silicone rubber presents yet a superior attribute under wet and polluted conditions compared to other materials, such as ethylene propylene diene monomer, ethylene vinyl acetate or epoxy. Silicone rubber exhibits hydrophobicity, which is responsible for inhibiting leakage current development. Although hydrophobicity may be temporarily lost due to prolonged wetting or corona, recovery takes place in a matter of hours once the stress is removed [1].

Once hydrophobicity is lost, a conductive water film is able to develop on the surface and dry band arcing may begin. It is known that dry band arcing degrades the polymeric weathershed due to the heat, ozone and UV generated by the discharges. Among these degradation factors, heat is the most harmful, leading to thermal decomposition of the polymer which further leads to tracking and erosion, and may bring the insulator to an electrical and eventually a mechanical failure [2]. Field results indicate that the main degradation factor of silicone rubber insulators exposed to a coastal environment is thermal depolymerization activated by electrical discharges [3].

Heat is a well known factor in the degradation of polymeric insulators under dry band arcing but very little has been done in terms of quantifying the thermal properties of such materials. In one of the early studies dealing with this subject, a model, employing thermal properties of the materials, was developed [2] and shows the relationship of the leakage current and temperature rise on the surface of an insulating material exposed to dry-band arcing. Sev-

eral studies also have reported on the effects of temperature, due to dry band arcing, in the degradation of polymeric insulating materials [4–8].

The present work addresses the relationship between thermal conductivity and the resistance to erosion under dry band arcing in the inclined plane test of silicone rubber containing various amounts and mean sizes of alumina tri-hydrate and silica fillers. Although many studies have been carried out to investigate the effect of fillers in composite insulators, the comparisons are made with different substrates and particle sizes of different values [9]. However, in this work, silicone rubber was used as base polymer in all samples, with ATH and silica as fillers. In addition, the mean particle sizes of $1.5\ \mu\text{m}$, $5\ \mu\text{m}$ and $10\ \mu\text{m}$ were chosen for both types of fillers. A laser based transient heat technique in conjunction with an IR camera was used to measure the thermal conductivity, as the setup was readily available in the laboratory. Alternatively there are other standard methods that can be used for thermal conductivity measurements [10]. The results clearly show that the increased filler concentration leads to higher thermal conductivity that can be correlated to the reduced erosion in the inclined plane test. Also, it was observed that the intrinsic thermal conductivity of fillers is less important than filler-matrix bonding, as the latter affects strongly the thermal conductivity of the composite, hence the resistance to erosion.

2 EXPERIMENTAL

2.1 INCLINED PLANE

2.1.1 TEST SAMPLES

2.1.1.1 RTV SILICONE RUBBER

A two-part room temperature vulcanized (RTV) silicone rubber is used as the base material (GE Silicones, RTV615, [11]), with silica and ATH as the fillers. It consists of 60-80% vinyl polydimethyl siloxane and 10-30% vinyl containing resin with no fillers added. Commercial silica and ATH, with no surface treatment of any kind, e.g. silanization, having mean particle sizes (number arithmetic average throughout this work) of about $1.5\ \mu\text{m}$, $5\ \mu\text{m}$, and $10\ \mu\text{m}$ sizes were added to the silicone polymer. Other physical properties of these fillers, e.g. surface area for ATH particles can be found in [12–13]. Also, particle size distribution, from manufacturer data sheets, can be found in [12–13] for ATH and in [14–16] for silica. A summary of the parameters relevant to Nielsen's thermal model [17], used to predict thermal conductivity of silicone rubber composites can be found in our earlier publication [18].

Test specimens were prepared using 10 %, 30 %, and 50 % of filler by weight (all filler percentages are given in wt% in this work). The prepared composites can also be compared in terms of their volume fraction, Table 1. The base silicone polymer and fillers were weighed accurately

Table 1. Comparison between filler concentration in terms of % weight and % volume for all samples tested.

	Weight (%) of ATH Filled Samples			Weight (%) of Silica Filled Samples		
	10	30	50	10	30	50
Volume Fraction (%)	4.5	15.3	29.7	4.1	14.2	27.8

and mixed thoroughly. After the addition of the curing agent, the mixture was stirred again, poured into a mould and degassed. Six samples were prepared for each compound and were cut to the appropriate size according to ASTM D2303 [19]. The surfaces of all the specimens were sanded with very fine sandpaper under tap water, washed with distilled water, and cleaned with isopropyl alcohol prior to testing.

Samples were cut from different locations and depths from the main mould and were examined under a scanning electron microscope and energy dispersive X-ray. The observations confirmed that the filler was dispersed uniformly throughout the sample.

2.1.1.2 HOT PRESSED SILICONE RUBBER

The hot pressed samples were prepared with same base polymer and fillers as the RTV samples. Silica and ATH were used at $1.5\ \mu\text{m}$, $5\ \mu\text{m}$, and $10\ \mu\text{m}$ mean particle size, however, at 30 and 50% concentrations. After mixing and degassing, the mixture was poured in a stainless steel mould, followed by the application of heat and pressure. The samples were held for one hour at $120\ ^\circ\text{C}$ and at an applied pressure of $0.5\ \text{kg}/\text{mm}^2$. The resulting compounds had a uniform thickness of $7 \pm 0.1\ \text{mm}$. Three samples of each compound were then prepared according to ASTM D2303.

2.1.2 SETUP AND PROCEDURE

The inclined plane test setup used in this work is shown in Figure 1 and has been previously described [20]. The test procedure follows ASTM D2303, with the initial volt-

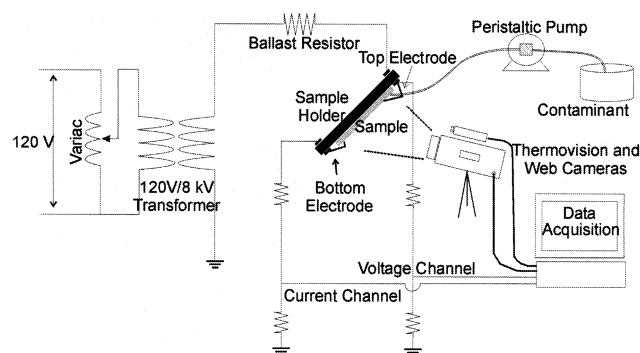


Figure 1. Simultaneous measurements of voltage, leakage current and temperature during the inclined plane test (ASTM D2303).

age of 2.0 kV and a constant contaminant flow rate of 0.15 ml/min for four hours. The test started when a stable stream of contaminant, flowing in the surface along the axial centre of each sample, was reached. At each hour the voltage was increased by 250 V. The samples were taken from the test bay and the eroded mass was estimated by filling the eroded volume with a known density material. The weight of the filling material was determined using a microbalance and used in the volume calculations. By knowing the density of the silicone rubber composite employed, the eroded mass was determined.

2.2 THERMAL CONDUCTIVITY

2.2.1 TEST SAMPLES

2.2.1.1 RTV SAMPLES

Samples made from two-part room temperature vulcanized silicone rubber filled with 10%, 30% and 50% of filler by weight were prepared using commercial grade ATH or silica (identical to those produced for the inclined plane tests). For each filler and concentration, three mean particle sizes were employed, 1.5 μm , 5 μm and 10 μm . Also, a small amount of FeO (0.4%) was added in order to provide a light red colour to the samples, favouring absorption of the near-infrared laser. In order to check the influence of iron oxide in the composite, samples were tested in inclined plane and, regarding eroded mass, minor differences can be seen between samples with and without iron oxide.

For each formulation, after weighting and mixing the proper amounts of silicone rubber and filler, the compound was poured into a mould and degassed following the manufacturer's recommendations. Heat was applied to accelerate the cure. After curing, disc shaped samples of 19mm diameter with a thickness of 9 ± 0.1 mm were prepared for the laser tests.

2.2.1.2 HOT PRESSED SAMPLES

The hot pressed samples for the thermal conductivity measurements were prepared in the same way as for the inclined plane test as described above. The samples were

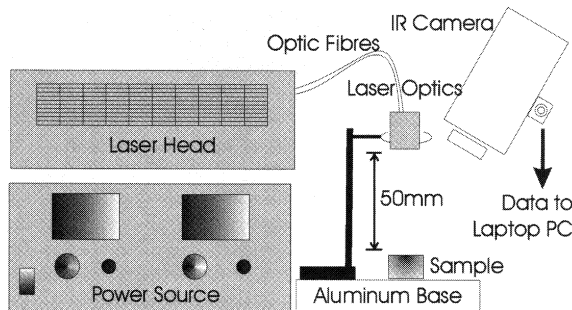


Figure 2. Laser setup for determining the thermal conductivity by measuring the temperature decay on samples [17].

cut from the sheets in a disc shape of 19 mm diameter with a thickness of 7 ± 0.1 mm. A small dot of silver/carbon black paint was applied to the surface of one of the samples to aid in the absorption of the heat energy from the laser source.

2.2.2 SETUP AND PROCEDURE

2.2.2.1 RTV SAMPLES

A 810 nm wavelength continuous near-infrared (NIR) semiconductor laser is used to heat the samples (Figure 2). Laser heating provides a contact free method and its output power is adjusted by varying the current. Unlike a UV laser, near-infrared laser develops only heat, without breaking polymer bonds. This was confirmed by observing the surface of the samples after exposure to the NIR laser source. The power used in these tests varied from 3 to 9 W.

For the RTV samples (iron oxide added), the surface of the samples was irradiated with the laser so as to produce a temperature ramp of 10.6 $^{\circ}\text{C}$ per second, reaching 212 $^{\circ}\text{C}$ in about 20 s. The temperature was then held at 212 $^{\circ}\text{C}$ for 1 minute, which was sufficient to achieve a steady state condition. The laser beam was then blocked, with the thermovision equipment recording the cooling profile of the samples until they reached 50 $^{\circ}\text{C}$.

2.2.2.2 HOT PRESSED SAMPLES

The same near-infrared laser used to test the RTV samples was used to determine the thermal conductivity of the hot pressed samples, although the procedure used was different. The samples were heated by applying a constant laser power of about 1.5 W to the silver/carbon black dot for a short time. The temperature transient on the opposite face of the sample, as illustrated in Figure 3, measured by the thermal imaging camera, was recorded until the temperature increased by 1 $^{\circ}\text{C}$. The thermal images for post-processing were recorded by a PC at a framing rate of 5 Hz.

Few samples were tested adopting both methods to measure the thermal conductivity and similar results were obtained; with less than 5% of difference. A summary of samples prepared and their corresponding use in the tests is shown in Table 2.

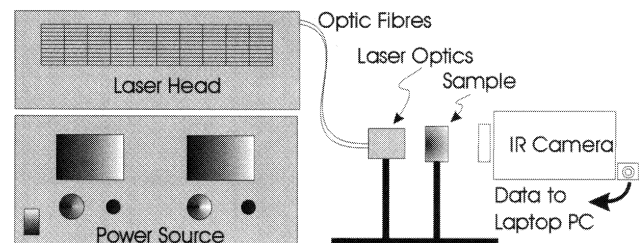


Figure 3. Laser setup for determining the thermal conductivity of samples based point source transient method [21].

Table 2. Summary of Samples Tested.

Process & Test Sample Characteristics	RTV Samples		Hot Pressed Samples	
	Inclined Plane	Thermal Conductivity	Inclined Plane	Thermal Conductivity.
Filler Mean Particle Size (μm)	1.5, 5 and 10	1.5, 5 and 10	1.5, 5 and 10	1.5, 5 and 10
Filler Concentration (wt %)	0, 10, 30 and 50	0, 10, 30 and 50	0, 30 and 50	0, 30 and 50
Sample Dimensions	ASTM D2303	19mm dia. 9mm \pm 0.1mm thickness	ASTM D2303	19mm dia. 5mm \pm 0.1mm thickness
Other		0.4 wt % FeO added		silver/carbon dot 2 mm dia painted on samples

2.3 THERMAL IMAGING CAMERA

A thermovision camera (SC500) was used to record the thermal response of the samples. The detector employs 7.5 to 13 μm emissivity spectra for temperature detection, averaging the emissivity over this wavelength. A 320×240 pixel array allows image composition, showing temperature distribution. The thermal sensitivity of the detector is 0.07 $^{\circ}\text{C}$ at 30 $^{\circ}\text{C}$ with an accuracy of $\pm 2^{\circ}\text{C}$ in the 23 to 500 $^{\circ}\text{C}$ range. The camera was connected to a PC running thermovision acquisition software, and the thermal images taken at 5 Hz were recorded.

To calibrate the emissivity of the top surface, the samples were placed in an oven for 2 hours to obtain a stable sample temperature. A thermocouple was used for the temperature measurement of the oven. The thermovision camera was focused on the samples and the emissivity in

the software was adjusted so that the camera indicated the same temperature as the thermocouple. As the emissivity was found not to significantly vary from sample to sample and in the range of the temperatures of interest, it was kept constant at 0.98.

3 RESULTS

3.1 INCLINED PLANE

3.1.1 RTV SAMPLES

The eroded mass of RTV and hot pressed samples subjected to the inclined plane test are shown in Table 3 and Table 4, respectively. In all tests, the samples lasted for four hours and there were no signs of puncture or tracking on any of the samples. Erosion occurred according to the amount of filler and the mean particle size, as seen in Table 3. Six samples of RTV silicone rubber without filler

Table 3. Eroded mass of RTV silicone rubber samples subjected to the inclined plane test.

Type	Filler		Eroded Mass (mg)		
	Concentration (wt %)	Mean Particle Size (μm)	Average	Mean	Standard Deviation
ATH	10	1.5	49.7	50.1	25.4
		5	17.1	17.1	5.0
		10	48.6	51.0	24.8
	30	1.5	12.1	12.3	2.6
		5	13.7	14.1	2.6
		10	20.9	21.5	4.6
	50	1.5	8.2	9.0	2.4
		5	9.7	8.8	3.0
		10	15.6	15.4	3.4
Silica	10	1.5	65.4	56.5	42.8
		5	95.4	73.8	51.4
		10	65.0	60.4	34.5
	30	1.5	10.6	7.6	8.4
		5	39.4	27.6	37.4
		10	89.4	18.6	121.6
	50	1.5	7.61	8.11	2.6
		5	9.9	9.9	2.2
		10	14.5	14.5	1.9

Table 4. Eroded mass of hot pressed silicone rubber samples subjected to the inclined plane test.

Type	Filler		Eroded Mass (mg)		
	Concentration (wt %)	Mean Particle Size (μm)	Average	Mean	Standard Deviation
ATH	30	1.5	20.3	19.9	12.8
		5	8.6	7.0	5.9
		10	17.2	15.7	9.2
	50	1.5	2.6	2.5	0.6
		5	2.5	2.4	0.5
		10	2.8	2.8	0.4
Silica	30	1.5	5.8	5.4	2.3
		5	6.0	6.0	1.8
		10	6.8	6.5	2.5
	50	1.5	2.6	2.5	0.5
		5	2.3	2.2	0.4
		10	1.7	1.8	0.3

were tested and the average mass loss was found to be 277 mg. It is evident from both figures that increasing the filler concentration improved the tracking and erosion resistance of the samples, even for a very low concentration of 10 %. With respect to particle size, there is no relationship between material mass loss and filler particle size at low filler concentration, i.e. at 10 % filler. Samples filled with large mean particle size showed the same mass loss as the samples filled with small particle size. Samples filled with 10 % ATH with 5 μm mean particle size performed well in the IPT test while on the other hand, samples filled with silica with a mean particle size of 5 μm performed badly.

The mass loss of samples loaded with 50 % ATH and silica decreased with decreasing mean particle size. A similar behaviour was found for the samples loaded with 30 % ATH and silica, although with 5 μm and 10 μm particles, the mass loss of samples with silica filler was much higher than ATH filled samples. In general, at low concentrations, 10 %, ATH filled samples performed better than samples filled with silica. However, at high concentrations, 50 %, both fillers showed similar results.

3.1.2 HOT PRESSED SAMPLES

As expected, the hot pressed samples subjected to the inclined plane test also demonstrated that increased filler concentration yields increased resistance to erosion, for both types of fillers, as seen in Table 4. However, a large spread in the results is evident among the samples filled with 30 % filler. The greatest resistance to erosion is shown by samples having filler with mean particle size of 5 μm , while 1.5 μm and 10 μm mean particle sizes show similar resistance. Samples filled with 50 % of ATH not only show a very low level of eroded mass, but also consistency in the results; whereas, the 5 μm mean filler samples show slightly higher resistance to erosion.

Among the samples filled with 30 % silica, 1.5 μm mean particle size show higher resistance to erosion, followed

by 5 μm and 10 μm mean particle sizes. At 50 % concentration, the ranking is the reverse of the ranking at 30 % concentration, with less eroded mass being shown by samples having 10 μm mean particle size silica, followed by samples having 5 μm and 1.5 μm means particle sizes.

In comparing the performance between ATH and silica filled samples, silica has shown higher resistance to erosion than ATH filled samples, in average, at both 30 % and 50 % concentrations.

3.2 THERMAL CONDUCTIVITY

3.2.1 RTV SAMPLES

3.2.1.1 TEMPERATURE DISTRIBUTION

The thermovision information for each sample was explored by means of the temperature profile along a line passing through the centre of the heated zone (line temperature profile). As the sample has a circular form, this profile will be the same for any line passing through the centre. In Figure 4 two images of temperature are shown, and, in Figure 5, their corresponding line temperature profiles are compared. The line temperature profile was recorded for all samples, including an un-filled one, 10 seconds after switching off the laser.

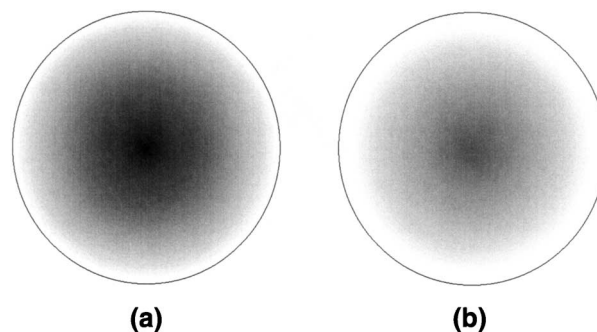


Figure 4. Typical temperature distribution on sample top surface. The darker regions represent higher temperatures. A, at $t = 0$; B, at $t = 10\text{s}$.

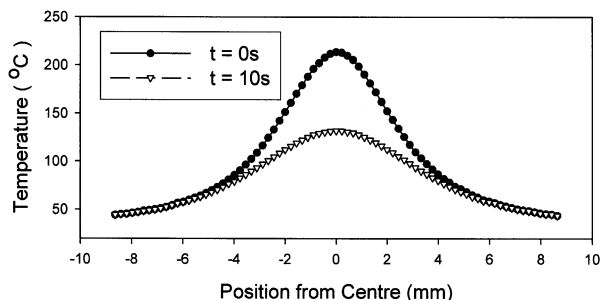


Figure 5. Temperature profiles along a line passing through the center of samples shown in Figures 6A and 6B.

Table 5 shows the maximum temperature recorded along the line temperature profile, for ATH and silica filled samples. The un-filled sample showed a maximum temperature of 154.5°C.

The maximum temperature along the line profile was taken after 10 s of switching off the laser, although the temperature after 5 and 15 s were also computed, which lead to similar temperature ratios with respect to the un-filled sample.

3.2.1.2 ESTIMATED THERMAL CONDUCTIVITY

If the maximum temperature of the line profile is plotted against time, an exponential decay curve is obtained. This decay curve (experimental data) is shown in Figure 6 for the un-filled sample, along with fitted expression and the residuals (difference between experimental data and fitted expression).

The curve presented in Figure 6 can be described by an empirical relationship:

$$T = T_R + T_0 \cdot e^{-\alpha \cdot t} \tag{1}$$

Assuming that $\alpha \propto k$ one can write $\alpha = C k$, where T_0 is the initial elevated temperature, T_R room temperature, k thermal conductivity and C a constant of proportionality for the exponent α .

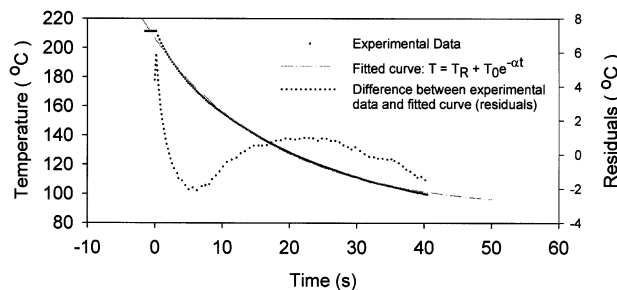


Figure 6. Temperature decay data, fitted curve and residuals for the unfilled sample.

As the thermal conductivity for un-filled silicone rubber is known from the manufacturer’s data sheet, for the un-filled sample the parameter “ C ” can be calculated as $C = \alpha/k$. By associating the decay temperature with thermal conductivity as shown by Equation 1, it is implicit that the only form of heat transfer acting on the sample during cooling is conduction, while radiation and convection are negligible due to their relatively small effects. Equation 1 was fitted to the temperature decay curve for all samples, from which the thermal conductivity “ k ” was extracted. Table 5 shows the estimated thermal conductivities for ATH and silica filled samples.

Measurement of thermal conductivity, following standard ASTM E1225-99 [9], was done for ATH and silica filled samples. Table 6 shows the measured k values for samples with both types of fillers at 10 and 50 % concentration with 1.5 μm particles, along with corresponding values from Table 5 for comparison. The thermal conductivities estimated based on the temperature profiles and Equation 1 show excellent agreement with the measured thermal conductivities, Tables 3 and 4. With the samples prepared under controlled conditions, it is observed from Table 3 that increased filler concentration results in increased thermal conductivities, as expected.

The effect of filler particle size between ATH and silica filled samples is seen in Table 5. In ATH filled samples, the highest thermal conductivity for the composite was

Table 5. Maximum temperature (°C) along the line temperature profile for ATH and silica filled samples, 10s after switching off the laser and estimated thermal conductivities, based on unfilled* sample.

Filler Concentration wt%	Maximum Temperature Along the Line Profile (°C)					
	Particle Size (μm) of ATH Filled Samples			Particle Size (μm) of Silica Filled Sample		
	1.5	5	10	1.5	5	10
10	130.7	122.2	136.4	120.3	127.2	127.6
30	100.8	99.1	106.1	97.4	104.8	106.4
50	88.73	85.1	87.9	84.2	88.1	92.3
Thermal Conductivity (W/m K)						
10	0.294	0.337	0.267	0.347	0.311	0.309
30	0.463	0.475	0.429	0.486	0.437	0.427
50	0.551	0.580	0.557	0.588	0.556	0.523

*-Unfilled sample has maximum temperature profile of 154.5 °C and a thermal conductivity of 0.19 W/m K.

Table 6. Measured (ASTM E1225-99) and estimated (Table 5) thermal conductivity (W/m K) for ATH and silica filled samples, employing 1.5 μm mean particle size.

Filler	Concentration	Measured (ASTM E1225-99)	Estimated
ATH	10%	0.29	0.294
	50%	0.551	0.57
Silica	10%	0.30	0.347
	50%	0.58	0.588

observed with 5 μm particles; whereas, with silica filled samples the finer the particles the higher the thermal conductivity of the composite. It is interesting to note the agreement with results previously published by Deng et al. [21].

In comparing ATH to silica, at 1.5 μm particle mean size, silica has led to higher thermal conductivity than ATH in all concentrations. At 5 μm, just the opposite is observed, with ATH yielding higher thermal conductivity than silica. At 10 μm particle size, the ranking is concentration dependent; at 10 % concentration, silica filled samples have better thermal conductivity, at 30 %, the thermal conductivities are comparable and at 50% ATH filled samples led to higher thermal conductivity. It should be noted that the estimated thermal conductivities have shown very good agreement with the measured thermal conductivities shown in Table 6, which were determined in accordance with the ASTM standard.

3.2.2 HOT PRESSED SILICONE RUBBER

A typical thermal transient of the sample temperature rise on the opposite side of the laser application side is shown in Figure 7. The effect of the boundary (convection and radiation) on the transient response was found insignificant up to a tested temperature rise of 3°C where the thermal transient model developed by Carslaw and Jaeger [22] for a continuous and constant point source of heat can be applied. The model describes the temperature rise *T* in a point at a distance *r* of the heat source *q*, at time *t*, as shown in equation (2).

$$T(t) = \frac{q}{4\pi\alpha r} \operatorname{erfc}\left(\frac{r}{\sqrt{4\alpha t}}\right) \quad (2)$$

where α is the thermal diffusivity of the material and *erfc* is the error function. Thus, the recorded transient temperature was curve fitted to the model described by equa-

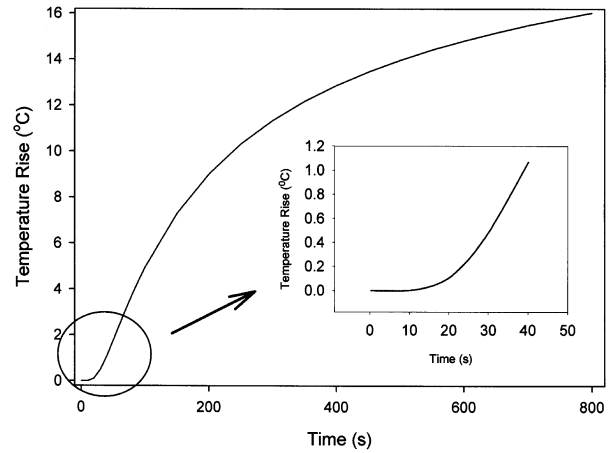


Figure 7. Overall typical temperature response of a sample with diffusivity of 0.15 mm²/s as a function of time, at a distance of 7mm from source, according to Carslaw and Jaeger [21] model for a constant and continuous point source of heat. The inserted graph shows temperature development in the initial region of interest.

tion (2), from which the thermal diffusivities were obtained. By knowing the densities and heat capacities of each sample, given by manufacturer’s data sheets and shown in Table 7, the thermal conductivities are obtained and are shown in Table 8 for both ATH and silica filled samples. It is clear that higher amount of filler has led to increased thermal conductivities. For ATH filled samples, at 30 % and 50 % concentrations, the higher thermal conductivities were found in samples that had employed 5 μm mean particle size. For silica filled samples at 30% concentration, there is little distinction of the thermal conductivities with respect to mean particle size. At 50 % concentration, increased particle size has led to increased thermal conductivities. In comparing ATH to silica filled samples, silica filled samples were found to have consistently higher thermal conductivities than ATH filled samples, despite the intrinsic higher thermal conductivity of ATH in comparison with silica.

Table 7. Densities and Heat capacities of the filled silicone rubber tested.

Filler	ATH		Silica	
	30%	50%	30%	50%
Concentration				
Density (g/mm ³)	0.0012	0.0013	0.0013	0.0014
Heat Capacity (J/g-K)	1.22	1.24	1.03	0.94

Table 8. Estimated thermal diffusivities and thermal conductivities for hot pressed ATH and silica filled samples.

Filler Concentration wt %	Thermal Diffusivity (mm ² /s)					
	ATH Filled Samples			Silica Filled Samples		
	1.5 μm	5 μm	10 μm	1.5 μm	5 μm	10 μm
30	0.26	0.27	0.26	0.34	0.34	0.32
50	0.44	0.46	0.31	0.54	0.63	0.73
	Thermal Conductivity (W/m K)					
30	0.37	0.39	0.39	0.46	0.46	0.43
50	0.71	0.75	0.50	0.71	0.83	0.97

Table 9. Correlation factors between measured eroded mass from incline plane test and thermal conductivity, RTV samples.

RTV Sample			Test		Correlation ($-1 \leq 0 \leq 1$) ^{1,2} [Significance] ²		
Filler	Wt%	Mean Particle Size (%)	IPT Erosion (mg)	Thermal Conductivity (W/m K)	By filler %	By Wt%	Overall
ATH	10	1.5	50.1	0.29	-0.97	-0.28	
		5	17.1	0.34			
		10	51.0	0.27			
Silica		1.5	56.5	0.35	-0.67	[0.60]	
		5	73.8	0.31			
		10	60.4	0.31			
ATH	30	1.5	12.3	0.46	-0.91	-0.82	-0.84
		5	14.1	0.47			
		10	21.5	0.43			
Silica		1.5	7.6	0.49	-0.91	[0.046]	[0.001]
		5	27.6	0.44			
		10	18.6	0.43			
ATH	50	1.5	9.0	0.55	-0.22	-0.61	
		5	8.8	0.58			
		10	15.4	0.56			
Silica		1.5	8.1	0.59	-0.95	[0.20]	
		5	9.9	0.55			
		10	14.5	0.52			

¹ As defined by Equation 3.

² Calculated by the SPSS statistical package [25].

4 DISCUSSION

The main factors acting towards material degradation, when subjected to dry band arcing are known to be the chemical reactions triggered by ozone, bond weakening due to UV from discharges and heat. Among these factors, heat is considered to play the major role, breaking the polymeric chains into smaller length chains, until final pyrolysis of the chain [6, 23]. Thus, a material having a high thermal conductivity would be able to conduct the heat away from the dry band zone faster than a material with lower thermal conductivity, increasing the erosion resistance and time to failure.

In order to further support the relationship between erosion resistance and thermal conductivity, the results were compared using correlation analysis. The correlation factor is given by [24]

$$C(Y_1, Y_2) = \frac{Cov(Y_1, Y_2)}{\sigma_{Y_1} \sigma_{Y_2}} \quad (3)$$

where Y_1 and Y_2 are the two sets of data. The covariance Cov is defined as $\frac{1}{N} \sum (Y_1(i) - \mu_{Y_1})(Y_2(i) - \mu_{Y_2})$, where μ_{Y_1} and μ_{Y_2} are the respective means of the data sets, with N points on both. The standard deviations are designated as σ_{Y_1} and σ_{Y_2} for Y_1 and Y_2 data sets, respectively. The correlation factor thus obtained is a real number within the limits $-1 \leq C(Y_1, Y_2) \leq 1$, where the extremes indicate a perfect linear relationship while a zero correlation factor indicates no correlation at all. The cor-

relation results for room temperature vulcanized samples are shown in Table 9 for RTV and hot pressed samples respectively.

From the analysis in Table 9 it is evident that extremely good correlation is shown for both ATH and silica filled samples, at all filler levels, with the one exception of RTV samples filled with ATH at 50 %. Excellent correlation is shown for samples filled with 10 % and 30 % of ATH, and 30% and 50 % of silica. In comparing the two filler types, 10 % concentration shows poorer correlation, while samples filled at 30 % and 50 % show good correlations. Overall, the correlation of thermal conductivity to eroded mass is much closer to unity than to the zero value. The negative correlation means that the higher the thermal conductivity, the lower the erosion. It is important to note that although the thermal conductivity was chosen as a thermal parameter to be correlated with erosion in inclined plane test, the thermal diffusivity is also a variable of interest. The thermal diffusivity expresses how fast the heat can travel and is, of course, related with thermal conductivity, heat capacity and density. Although an electrical discharge is, by nature, a fast phenomenon, the continuous dry band arcing in the inclined plane test and its thermal implications can be considered a relatively slow phenomenon; hence the thermal conductivity was chosen for the correlation analysis with erosion in inclined plane test.

Table 10 shows the correlation factors for hot pressed samples. Except for samples filled with ATH at 30% concentration, all other correlation factors are exceptionally good, approaching the perfect linear relationship. Despite

Table 10. Correlation factors between measured eroded mass from inclined plane test and thermal conductivity, hot pressed samples.

Hot Pressed Samples			Test		Correlation ($-1 \leq 0 \leq 1$) ^{1,2} [Significance] ²		
Filler	Wt%	Mean Particle (μm)	IPT Erosion (mg)	Thermal Conductivity (W/m K)	By filler and %	By Wt%	Overall
ATH	30	1.5	19.9	0.37	-0.75	-0.80	
		5	-7.0	0.39			
		10	15.7	0.39			
Silica	30	1.5	5.4	0.46	-0.84	[0.056]	
		5	6.0	0.46			
		10	6.5	0.43			
ATH	50	1.5	2.5	0.71	-0.996	-0.98	[0.014]
		5	2.4	0.75			
		10	2.8	0.50			
Silica	50	1.5	2.5	0.71	-0.999	[0.005]	
		5	2.2	0.83			
		10	1.8	0.97			

¹ As defined by Equation 3.² Calculated by the SPSS statistical package [25].

its bad ranking within the group, ATH filled samples at 30% concentration show better positioning among all 30% filled samples, which includes silica filled samples as well, where the correlation factor has reached -0.80 . The same good correlation factor is seen at 50% filled samples, for both ATH and silica, reaching a value of -0.98 . The overall correlation, including all samples is consistent with samples prepared under RTV process, reaching a correlation factor of -0.68 .

Table 9 and Table 10 have shown the correlation factors for RTV and hot pressed samples, along the Pearson's significance test, shown in square brackets, which expresses the probability of being in error by rejecting the hypothesis that the correlation factor is zero. It can be seen that, for the overall analysis of the correlation, the correlation is significant to the 0.01 level for RTV samples and is significant to the 0.05 level for hot pressed samples, which means that the probability of the correlation being zero is very low, below 1% and 5%, respectively. The significance test was not performed inside each group of samples because of the low number of paired data.

Another aspect deals with materials employing flame retardants, like ATH for example, which would be capable to absorb more heat without damaging the polymeric bonds, due to the inherent higher enthalpy, provided by the water of hydration, not present in silica filled materials. On the other hand, silica has better bonding, implying in a higher mechanical strength, also imparting tracking and erosion resistance. The different nature of both ATH and silica fillers leads to different mechanisms of erosion resistance, ATH having the water of hydration and silica having better bonding to main polymer backbone, is also reflected by the correlation factors, as seen in Table 11. The correlation factors for all ATH and all silica filled samples are higher than the combined correlation factor, for both RTV and hot pressed samples.

Table 11. Summary of correlation factors for both all-only-ATH and all-only-silica filled samples, compared to correlation factor for all samples, taken from Tables 9 and 10.

Samples	Correlation ^{1,2} factor		
	ATH Filled	Silica filled	ATH & Silica
RTV	-0.86	-0.87	-0.84
Hot Pressed	-0.76	-0.96	-0.68

¹ As defined by equation (3).² Calculated by the SPSS statistical package [25].

It is interesting to note that despite an intrinsic thermal conductivity of about 15 times higher than the thermal conductivity of silica, ATH samples do not exhibit higher thermal conductivities than silica. In fact, silica filled samples have shown a higher average thermal conductivity than ATH among all of the samples, suggesting that other factors, for example, filler bonding, plays a bigger role than intrinsic thermal conductivity. A scanning electron microscope study was conducted to verify the bonding of filler particles to the polymeric matrix and photographs were taken for all composites. It was observed that ATH samples had many more weak bonding areas than silica filled samples. Typical images are shown in Figures 8 and 11, for ATH and silica filled samples, at 50% concentration, employing 1.5 μm mean particle size, in both methods of preparation employed. Higher resolution photographs, Figures 10 and 13, of hot pressed samples filled with 50% of ATH and silica, employing 10 μm mean particle size, highlight the weak bonding areas on ATH filled samples (Figure 10) and identify a better bonding of the silica particles with the main polymer (Figure 11), in silica filled samples. The main observed difference is that, while ATH particles may be sitting in their moulded cavity, silica particles are embedded in the silicone rubber polymeric matrix, thus increasing thermal conductivity and resistance to erosion.

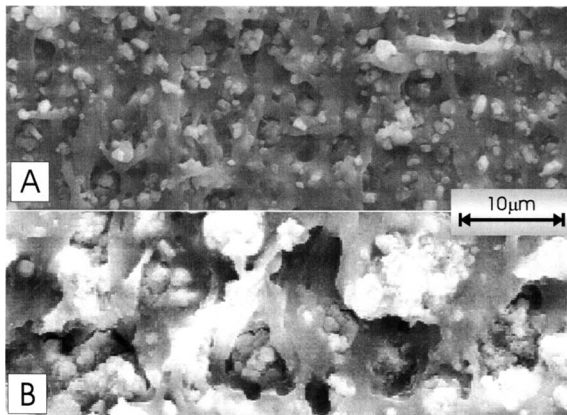


Figure 8. Scanning electron microscope photographs showing a sample filled with 50 wt% of ATH using $1.5 \mu\text{m}$ mean particle size. A, hot pressed sample; B, RTV silicone rubber.

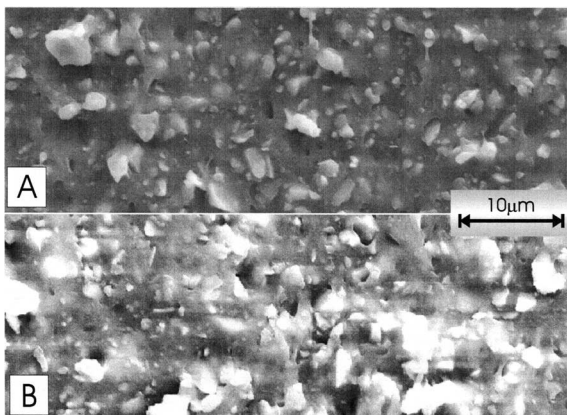


Figure 9. Scanning electron microscope photographs showing a sample filled with 50 wt% of silica using $1.5 \mu\text{m}$ mean particle size. A, hot pressed sample; B, RTV silicone rubber.

5 CONCLUSIONS

FROM the results and discussion presented in the previous sections, the following conclusions can be made:

- A correlation study has shown that the resistance to erosion due to dry band arcing of silicone rubber composites, filled with ATH or silica, are strongly correlated to the thermal conductivity of the composite.
- Higher filler concentrations in silicone rubber composites result in increased thermal conductivities and thus higher resistance to erosion due to dry band arcing, for both RTV and hot press employed processes.
- The thermal conductivity of ATH or silica filled silicone rubber is very sensitive to the filler ability to bond to the polymeric matrix, showing, among the fillers, concentrations and mean particle sizes tested, to be of more importance than the filler's intrinsic thermal conductivity.
- ATH filled samples, at 10 wt% and 30 wt% concentrations, have higher erosion resistance and thermal con-

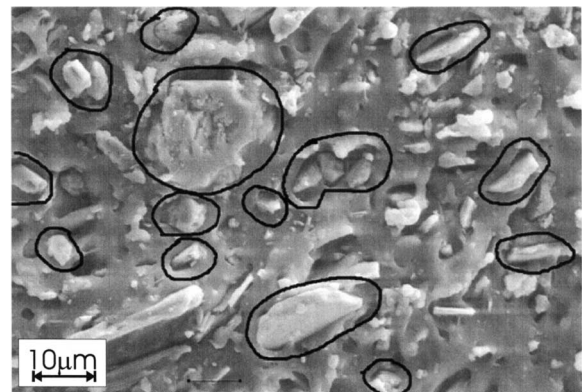


Figure 10. Scanning electron microscope of a sample containing 50 wt% of ATH, with $10 \mu\text{m}$ mean particle size. Selected areas show weak bonding of the filler particle to the main polymeric matrix.

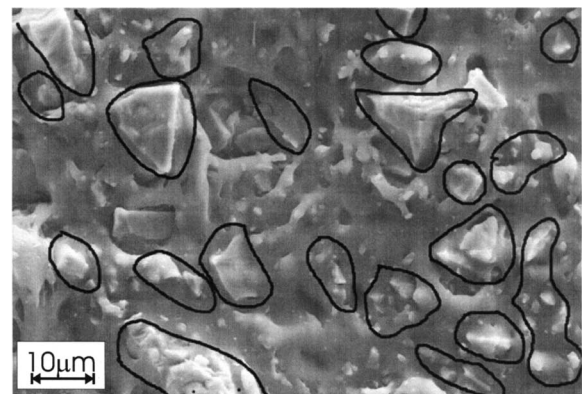


Figure 11. Scanning electron microscope of a sample containing 50 wt% of silica, with $10 \mu\text{m}$ mean particle size. Selected areas show good bonding of the filler particle to the main polymeric matrix.

ductivity than the corresponding silica filled samples, in RTV silicone, while at 50 wt% both have quite similar resistance to erosion where silica filled samples show slightly better performance.

- Hot pressed samples employing silica as filler have higher thermal conductivity and resistance to erosion due to dry band arcing than samples filled with ATH, for the concentrations (30 and 50 wt%) and particle sizes (1.5, 5, and $10 \mu\text{m}$) tested.
- Hot pressed samples filled with ATH and silica have higher thermal conductivity and resistance to erosion due to dry band arcing than room temperature vulcanized samples.

ACKNOWLEDGMENTS

The financial support provided by NSERC (Natural Sciences and Engineering Research Council of Canada) is appreciated. One of the authors, Luiz Meyer, gratefully acknowledges CAPES (Brazilian Research Agency for Post-Graduate Education) and FURB (University of Blumenau) for financially supporting his graduate studies. The

authors would like to acknowledge Dr. V. Grishko and Dr. W. W. Duley, Department of Physics, University of Waterloo, for their support on the laser experiments. The authors are also grateful to the anonymous reviewers for their critical comments that were very useful in enhancing the quality of this paper.

REFERENCES

- [1] S. H. Kim, E. A. Cherney, R. Hackam and K. G. Rutherford, "Chemical Changes at the Surface of RTV Silicone Rubber Coatings on Insulators During Dry-Band Arcing", *IEEE Trans. Dielectr. Electr. Insul.*, Vol. 1, pp. 106–123, 1994.
- [2] R. S. Gorur, E. A. Cherney and R. Hackam, "The AC and DC Performance of Polymeric Insulating Materials under Accelerated Aging in a Fog Chamber", *IEEE Trans. Power Delivery*, Vol. 3, pp. 1892–1902, 1988.
- [3] T. G. Gustavsson, S. M. Gubansky, H. Hillborg, S. Karlson and U. W. Gedde, "Aging of Silicone Rubber under AC or DC Voltages in a Coastal Environment", *IEEE Trans. Dielectr. Electr. Insul.*, Vol. 8, pp. 1029–1039, 2001.
- [4] S. H. Kim, E. A. Cherney and R. Hackam, "Thermal Characteristics of RTV Silicone Rubber Coating as a Function of Filler Level", *IEEE-CEIDP*, pp. 713–718, 1992.
- [5] S. H. Kim and R. Hackam, "Temperature Distribution in RTV Silicone Rubber Following Dry-Band Arcing", *IEEE-ISEI*, Pittsburgh, pp. 599–602, 1994.
- [6] S. Kumagai and N. Yoshimura, "Tracking and Erosion of HTV Silicone Rubber and Suppression Mechanism of ATH", *IEEE Trans. Dielectr. Electr. Insul.*, Vol. 8, pp. 203–211, 2001.
- [7] S. Kumagai and N. Yoshimura, "Tracking and Erosion of HTV Silicone Rubbers of Different Thickness", *IEEE Trans. Dielectr. Electr. Insul.*, Vol. 8, pp. 673–678, 2001.
- [8] H. Homma, T. Kuroyagi, K. Izumi, C. L. Mirley, J. Ronzello and S. A. Boggs, "Evaluation on Surface Degradation of Silicone Rubber Using Thermogravimetric Analysis", *Symposium on Electrical Insulating Materials*, Toyohashi, Japan, pp. 631–634, 1998.
- [9] R. Hackam, "Outdoor HV Composite Polymeric Insulators", *IEEE Trans. Dielectr. Electr. Insul.*, Vol. 6, pp. 557–585, 1999.
- [10] ASTM E 1225-99, "Standard Test Method for Thermal Conductivity of Solids by Means of the Guarded-Comparative-Longitudinal Heat Flow Technique, 1999.
- [11] GE Silicones; "RTV 615 Data Sheet", General Electric Company 2003.
- [12] Alcan Chemicals; Data Sheet 100 – Aluminium Trihydroxide FRF Grades", 1999.
- [13] Alcan Chemicals; "Data Sheet 141 – Aluminium Trihydroxide SF Grades", 1999.
- [14] U.S. Silica Company, "Min-U-Sil-5 Product Data Sheet", 1999.
- [15] U.S. Silica Company, "Min-U-Sil-15 Product Data Sheet", 1999.
- [16] U.S. Silica Company, "Min-U-Sil-40 Product Data Sheet", 1999.
- [17] L. E. Nielsen, *Mechanical Properties of Polymers and Composites*, NY, USA, Marcel Dekker, 1974.
- [18] L. Meyer, V. Grishko, S. Jayaram, E. Cherney and W. W. Duley, "Thermal Characteristics of Silicone Rubber Filled with ATH and Silica under Laser Heating", *Conf. Electr. Insul. Dielectr. Phenomena*, Cancun, Mexico, pp. 848–852, 2002.
- [19] ASTM-D2303, "Standard Test Method for Liquid-Contaminant, Inclined-Plane Tracking and Erosion of Insulating Materials".
- [20] L. Meyer, R. Omranipour, S. Jayaram and E. Cherney, "The Effect of ATH and Silica on Tracking and Erosion Resistance of Silicone Rubber Compound for Outdoor Insulation", *ISEI*, pp. 271–274, 2002.
- [21] H. Deng, R. Hackam and E. A. Cherney, "Role of Size of Particles of Alumina Trihydrate Filler on the Life of RTV Silicone Rubber Coating", *IEEE Trans. Power Delivery*, Vol. 10, pp. 1012–1024, 1995.
- [22] S. Carslaw and J. C. Jaeger, *Conduction of Heat in Solids*, Oxford Press, London, 1959.
- [23] G. Camino, S. M. Lomkin and M. Lazzari, "Polydimethylsiloxane Thermal Degradation. Part 1. Kinetic Aspects", *Elsevier Polymer*, No. 42, pp. 2395–2402, 2001.
- [24] J. Miles and M. Shevlin; "Applying Regression & Correlation: A Guide for Students and Researchers". Thousand Oaks, Calif., Sage Publications, 2001.
- [25] SPSS Inc., *SPSS User Guide*, 2003.



Luiz Henrique Meyer (S'93) was born in Blumenau, SC, Brazil in April 1968. He received the B.S. and M.S. degrees in electrical engineering from the Universidade Federal de Santa Catarina, Florianópolis, Brazil, in 1991 and 1994, respectively and the Ph.D. degree in Electrical Engineering from the University of Waterloo in 2003. He joined the Electrical Engineering Dept. of the Universidade Regional de Blumenau, Blumenau, Brazil, in 1993 where he has been involved with academic and research activities. From 1998 to 2000 he was Director of the Technological Research Institute of the Universidade Regional de Blumenau, Blumenau, Brazil. He is currently on study leave at the University of Waterloo, Waterloo. His areas of research interest are high voltage engineering, polymeric insulating materials, and power apparatus.



Shesha H. Jayaram is a Professor in the Electrical and Computer Engineering Dept, University of Waterloo, Waterloo, and an Adjunct Professor at the University of Western Ontario, London. She received the B.A.Sc. degree in electrical engineering from the Bangalore University, the M.A.Sc. degree in high voltage engineering from the Indian Institute of Science, Bangalore, and the Ph.D. degree in electrical engineering from the University of Waterloo, in 1980, 1983, and 1990 respectively. Prof. Jayaram's research interests are developing diagnostics to analyze insulating materials, industrial applications of high voltage engineering, and applied electrostatics. Prof. Jayaram has been an active member of the IEEE Dielectric and Electrical Insulation Society and the Electrostatic Processes Committee (EPC) of the IEEE Industry Applications Society. In both, she has contributed as a board member, chair of EPC during 1998-99, session organizer/chair and as a member of the paper review process committee. She is a registered professional engineer in the province of Ontario, Canada.



Edward A. Cherney (M'73-SM'83-F'97), received the B.Sc. degree from the University of Waterloo, the M.Sc. degree from McMaster University and the Ph.D. degree from the University of Waterloo in 1967, 1969 and 1974, respectively. In 1968 he joined the Research Division of Ontario Hydro and in 1988 he went into manufacturing of polymer insulators and of silicone materials. Since 1999 he has been involved in international projects in outdoor insulation. He has been an adjunct professor for 22 years, first at the University of Windsor and currently at the University of Waterloo. He has published extensively, holds several patents, co-authored a book on outdoor insulators, actively involved in IEEE working groups, a registered engineer in the province of Ontario, and a Fellow of the IEEE.